

The influence of acidic and alkaline precursors on Pt–Ru/C catalyst performance for a direct methanol fuel cell

Zhen-Bo Wang*, Ge-Ping Yin*, Peng-Fei Shi

Department of Applied Chemistry, Harbin Institute of Technology, Harbin 150001, China

Received 20 July 2006; received in revised form 21 September 2006; accepted 27 September 2006

Available online 9 November 2006

Abstract

This research aims to increase the activity of platinum–ruthenium alloy (Pt–Ru/C) catalysts for methanol electrooxidation. The direct methanol fuel cell (DMFC) anodic Pt–Ru/C catalysts were prepared from acidic and alkaline $\text{Pt}(\text{NH}_3)_2(\text{NO}_2)_2$ solutions as Pt precursors, respectively, and with the same acidic Ru compound but without Cl^- ion as the Ru precursor by thermal reduction. The phase structures, lattice parameters, particle sizes, alloy composition, distribution, and the morphology of reduced catalysts were determined by means of X-ray diffraction (XRD), energy-dispersive analysis of X-ray (EDAX), and high-resolution transmission electron microscopy (TEM). It was found that the XRD patterns of the two catalysts showed Pt reflections for a face centered cubic (fcc) crystalline alloy structure. The catalyst prepared from the acidic $\text{Pt}(\text{NH}_3)_2(\text{NO}_2)_2$ as a precursor has a more homogeneous distribution of Pt–Ru metal particles on carbon. Its size is relatively small, about 3.7 nm. Its chemical composition is quite similar to theoretical value of 1:1 (Pt:Ru). The catalyst prepared from the alkaline $\text{Pt}(\text{NH}_3)_2(\text{NO}_2)_2$ as a precursor has an uneven distribution of Pt–Ru particles on carbon and its size is relatively large, and the chemical composition of Pt and Ru was 6:4. The performance was tested using a glassy carbon working electrode by cyclic voltammetry (CV) and chronoamperometric curves in a solution of 0.5 mol L^{-1} CH_3OH and 0.5 mol L^{-1} H_2SO_4 at 25°C . The electrocatalytic activity of the Pt–Ru/C catalyst prepared from the acidic $\text{Pt}(\text{NH}_3)_2(\text{NO}_2)_2$ as a precursor was the higher for methanol electrooxidation than that of catalyst from the alkaline source. The peak current density from the CV plot was 11.5 mA cm^{-2} .

© 2006 Elsevier B.V. All rights reserved.

Keywords: Direct methanol fuel cell; Acidic and alkaline Pt precursors; Pt–Ru/C catalyst; Methanol electrooxidation; Electrocatalytic activity

1. Introduction

In the past decades, the direct methanol fuel cell (DMFC) has been receiving increasing attention as a future power source for small portable electronic devices, such as laptops and mobile telephones, due to its advantages of fuel storage, simple structure, reduced system weight, high energy efficiency and low emissions [1–3]. DMFC is also regarded as one of most promising energy technologies for the 21st century. At present, Pt–Ru alloy and Pt metal are usually used as the anode and cathode catalysts for the DMFC, respectively. However, platinum and ruthenium are noble metals and have a low natural

abundance, which is a drawback for this catalyst for practical uses. It increases its cost and restricts its industrialization. Although Pt–Ru alloys are still considered to be the best catalysts because of their tolerance to CO formed as one of the intermediates of methanol electrooxidation, the activity of Pt–Ru alloy catalysts cannot satisfy with the performance requirement of DMFC, especially at low temperatures. Thus, there is a need to improve the activity of Pt–Ru alloy catalysts for methanol electrooxidation [4–6]. The activity of Pt–Ru catalysts is influenced by many factors such as the preparation methods and the technology [7–9]. Their preparation methods are dependent on the precursors, which markedly influenced the performance of the catalysts [10]. At present, Pt–Ru catalysts were usually prepared by chemical reduction with H_2PtCl_6 and RuCl_3 as the precursors. The Pt–Ru metal and carbon support may be eroded by the residual chloride ions from the precursors [11], thus its performance decays evidently. So, the Pt–Ru/C alloy catalysts were prepared by using the precursors without

* Corresponding author. Present address: Department of Chemistry, University of Puerto Rico, Rio Piedras Campus, San Juan, Puerto Rico 00931, United States. Tel.: +86 451 86402571; fax: +86 451 86402576.

E-mail addresses: wangzhenbo1008@yahoo.com.cn (Z.-B. Wang), yingphit@hit.edu.cn (G.-P. Yin).

Cl^- ions, such as $\text{Na}_6\text{Pt}(\text{SO}_3)_4$ and $\text{Na}_6\text{Ru}(\text{SO}_3)_4$. The performance was improved to a great extent [12]. The $\text{Pt}(\text{NH}_3)_2(\text{NO}_2)_2$ compounds are often used as a precursor of Pt-based catalysts. However, the $\text{Pt}(\text{NH}_3)_2(\text{NO}_2)_2$ compounds may form two solutions—acidic and alkaline, respectively.

In this work, the acidic and the alkaline $\text{Pt}(\text{NH}_3)_2(\text{NO}_2)_2$ compounds as Pt precursors and the same acidic Ru compound without Cl^- ion, was used as the Ru precursor. Vulcan XC-72 carbon black was used as a support for the catalyst. The Pt–Ru/C catalysts were prepared by thermal reduction. The effect of the acidic and the alkaline platinum compound precursors on catalyst performance was studied. Various characterization methods, such as X-ray diffraction (XRD), transmission electron microscopy (TEM), energy-dispersive analysis of X-ray (EDAX), CO stripping voltammetry, cyclic voltammetry (CV) and chronoamperometry (CA) curves were employed in conjunction with the activity test.

2. Experimental

2.1. Preparation of catalysts

The Pt–Ru/C catalysts were prepared according to the method from the literature [13]. As described briefly, carbon black powder (Vulcan XC-72) was used as a support for the catalyst. The samples containing 20% in weight of catalyst were dispersed on the carbon. The 0.25 g Pt–Ru (with an atomic ratio of 1:1)/C catalysts were obtained by thermal reduction. The acidic $\text{Pt}(\text{NH}_3)_2(\text{NO}_2)_2$ compound was from Ishifuku Metal Industry in Japan, and the alkaline $\text{Pt}(\text{NH}_3)_2(\text{NO}_2)_2$ and the acidic Ru compound without Cl^- ion were from China. The carbon black was dispersed in ultra-pure water and isopropyl alcohol ultrasonicated for 20 min. Then the precursors were added to the ink ultrasonically for 20 min. The pH value of the ink was measured by the pHS-25 acidity instrument. The ink was dried with a magnetic stirrer at 60 °C. The dried $\text{Pt}(\text{NH}_3)_2(\text{NO}_2)_2$ and Ru compounds with carbon was put into a tube furnace and reduced with a gaseous mixture of H_2 and Ar with an atomic ratio of 1:9. The catalyst powder was stored in a vacuum vessel.

2.2. Preparation of working electrode and its electrochemical measurements

2.2.1. Preparation of working electrode

Glassy carbon working electrodes (3 mm diameter; electrode area 0.0706 cm^2), polished with $0.05 \mu\text{m}$ alumina to a mirror-finish before each experiment, were used as substrates for the Vulcan-supported catalysts. For the electrode preparation, $5 \mu\text{L}$ of an ultrasonically redispersed catalyst suspension was pipetted on to the glassy carbon substrate. After the solvent evaporation, the deposited catalyst ($28 \mu\text{g}_{\text{metal}} \text{ cm}^{-2}$) was covered with $5 \mu\text{L}$ of a dilute aqueous Nafion solution. The resulting Nafion film with a thickness of $\leq 0.2 \mu\text{m}$ has a sufficient strength to attach the Vulcan particles permanently to the glassy carbon electrode without producing significant film diffusion resistances [14].

2.2.2. Electrochemical measurements

Electrochemical measurements were carried out in a conventional three-electrode electrochemical cell at 25 °C. The glassy carbon electrode as a working electrode (electrode area 0.0706 cm^2) was covered with catalyst powder. A piece of Pt foil of 1 cm^2 area was used as the counter one. A reversible hydrogen electrode (RHE) was used as the reference, which was connected to the working electrode compartment by a Luggin capillary whose tip was placed close to the working electrode. All potential values are vs. RHE. All chemicals used were of analytical grade. All the solutions were prepared with ultra-pure water (MilliQ, Millipore, $18.2 \text{ M}\Omega \text{ cm}$). A solution of $0.5 \text{ mol L}^{-1} \text{ CH}_3\text{OH}$ and $0.5 \text{ mol L}^{-1} \text{ H}_2\text{SO}_4$ was stirred constantly and purged with ultra-pure argon gas. Electrochemical experiments were performed using a CHI630A electrochemical analysis instrument. Cyclic voltammograms (CV) were taken at potentials ranging from 0.05 to 1.2 V. The scanning rate was 0.02 V s^{-1} . The chronoamperometric experiments were carried out using the CHI630A electrochemical analysis instrument controlled by a PC. The potential was stepped from 0.1 to 0.8 V. Due to a slight contamination from the Nafion film, the working electrodes were cycled at 0.05 V s^{-1} until the reproducible CV plots were obtained before the measurement curves were recorded.

2.2.3. CO stripping voltammetry

The electrode was electrochemically cleaned in an Ar-degassed solution of $0.5 \text{ mol L}^{-1} \text{ H}_2\text{SO}_4$ solution at 25 °C. The amount of Pt–Ru/C catalyst as the working electrode was $10 \mu\text{g}$ ($28 \mu\text{g}_{\text{metal}} \text{ cm}^{-2}$). CO was adsorbed on the surface of the Pt–Ru/C catalyst at 0.08 V by bubbling CO gas through the $0.5 \text{ mol L}^{-1} \text{ H}_2\text{SO}_4$ solution for 25 min. The CO dissolved in the solution was subsequently removed by bubbling argon gas of high purity for 35 min, keeping the potential also at 0.08 V. The potential was then cycled at a scanning rate of 0.02 V s^{-1} from 0.05 to 1.2 V for two oxidation and reduction cycles.

2.3. Physical measurements

2.3.1. X-ray diffraction (XRD) measurements

XRD analysis was carried out for the Pt–Ru/C catalysts from different precursors with a D/max-rB (Japan) diffractometer using a Cu $\text{K}\alpha$ source operating at 45 kV and 100 mA. The XRD patterns were plotted at a scanning rate of 4° min^{-1} with an angular resolution of 0.05° for 2θ scan.

2.3.2. Transmission electron micrographs (TEM)

Transmission electron micrographs for the catalyst samples were taken in a Japan JEOLJEM-1200EX Transmission Electron Microscope with a spatial resolution of 1 nm. Before taking the electron micrographs, the catalyst samples were finely ground and ultrasonically dispersed in isopropyl alcohol, and a drop of the resultant dispersion was deposited and dried on a standard copper-grid coated with a polymer film. The applied voltage was 100 kV with a magnification of 200,000 for the catalyst.

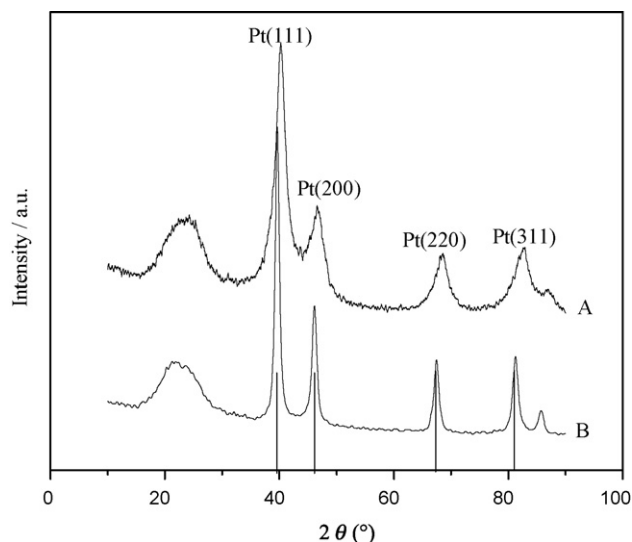


Fig. 1. XRD patterns of Pt–Ru/C catalysts prepared from the acidic (A) and the alkaline (B) $\text{Pt}(\text{NH}_3)_2(\text{NO}_2)_2$ as precursors.

2.3.3. Energy-dispersive analysis of X-ray (EDAX)

Chemical composition analysis by EDAX was performed with an EDAX Hitachi-S-4700 analyser associated to a scanning electron microscope (SEM, Hitachi Ltd., S-4700). Incident electron beam energies from 3 to 30 keV had been used. In all cases, the beam was at normal incidence to the sample surface and the measurement time was 100 s. All the EDAX spectra were corrected by using the ZAF correction, which takes into account the influence of the matrix material on the obtained spectra.

3. Results and discussion

3.1. Effect of precursors on crystalline structures and compositions of the catalysts

Fig. 1 shows the X-ray diffraction (XRD) patterns of the Pt–Ru/C catalysts prepared from the acidic (A) and the alkaline (B) $\text{Pt}(\text{NH}_3)_2(\text{NO}_2)_2$ solutions as Pt precursors at 360°C for 2 h. It can be seen that the first peak in the low 2θ range refers to the carbon support. The other four peaks are characteristic of face centered cubic (fcc) crystalline Pt (JCPDS-ICDD, Card No. 04-802), corresponding to the planes (1 1 1), (2 0 0), (2 2 0) and (3 1 1) at 2θ values of about 39.8° , 46.5° , 67.8° and 81.2° , respectively, indicating that the two catalysts have principally single-phase disordered structures (*i.e.* solid solutions). Comparing with the reflections of pure Pt (cf. the vertical lines of Pt in Fig. 1, referring to the Joint Committee on Powder Diffraction Data (JCPDS-ICDD) database), the diffraction peaks for the Pt–Ru catalysts are shifted slightly to the higher 2θ values.

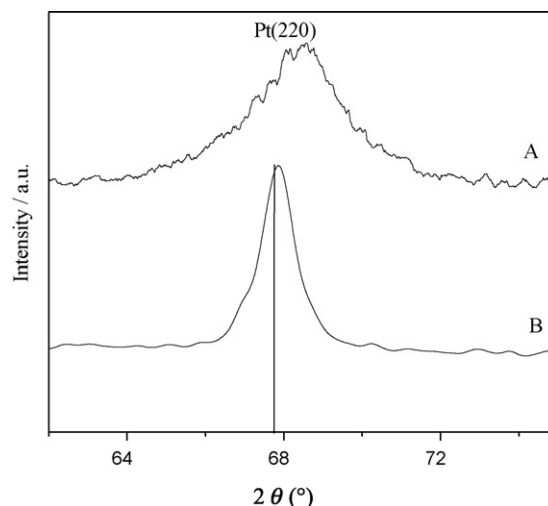


Fig. 2. XRD patterns of Pt–Ru/C catalysts prepared from the acidic (A) and the alkaline (B) $\text{Pt}(\text{NH}_3)_2(\text{NO}_2)_2$ as precursors in the 2θ range of $62\text{--}75^\circ$.

The slight shifts of the diffraction peaks reveal the formation of an alloy involving the incorporation of Ru atoms into the fcc structure of Pt. It is important to note that the diffraction peaks indicating the presence of either pure Ru or Ru-rich hexagonal close packed (hcp) phase do not appear, which suggests that Ru atoms either form an alloy with Pt or exist as oxides in amorphous phases.

Fig. 2 shows that the X-ray diffraction (XRD) patterns in the 2θ range of $62\text{--}75^\circ$ of the catalyst prepared from the acidic (A) and the alkaline (B) $\text{Pt}(\text{NH}_3)_2(\text{NO}_2)_2$ solutions. Comparing with the reflections of pure Pt (cf. the vertical lines of Pt in Fig. 2), it can be displayed that the diffraction peaks for the Pt–Ru catalysts are evidently shifted to the higher 2θ values. Its difference which the diffraction peaks are shifted in the XRD patterns, results in different alloying degree.

Because Ru atomic radius is smaller than that of Pt atom, following on Vegard's law, the lattice parameters of Pt–Ru/C catalysts decrease when Ru atoms incorporate into the fcc structure of Pt. In fact, the decrease in lattice parameters of the alloy catalysts reflects the progressive increase in the incorporation of Ru into the alloyed state. The diffraction peaks at Pt(2 2 0) at 68° were used to calculate the lattice parameters of Pt–Ru/C catalysts due to their peaks at Pt(1 1 1), (2 0 0) and (3 1 1) overlap the peaks of carbon support at about 43° and 82° . The lattice parameters and d values of the Pt–Ru/C catalysts are given in Table 1. The lattice parameters and d values of the two Pt–Ru/C catalysts are smaller than those for Pt/C. The decrease in lattice parameter of Pt–Ru/C catalyst from the acidic $\text{Pt}(\text{NH}_3)_2(\text{NO}_2)_2$ solution is more than that of from the alkaline one. It reveals that the alloying degree of the former is the higher one.

Table 1
Structural parameters and compositions of the Pt/C and Pt–Ru/C catalysts prepared from the acidic (A) and the alkaline (B) $\text{Pt}(\text{NH}_3)_2(\text{NO}_2)_2$ as precursors

(1 1 1) Plane	2θ ($^\circ$)	d -Value (nm)	Lattice parameter (nm)	Estimated Pt/Ru atomic ratio (at.%)
Pt/C	67.73	0.13873	0.3924	(100)
Pt–Ru/C (A)	68.24	0.13711	0.3878	53.2:46.8
Pt–Ru/C (B)	67.91	0.13793	0.3901	61.8:38.2

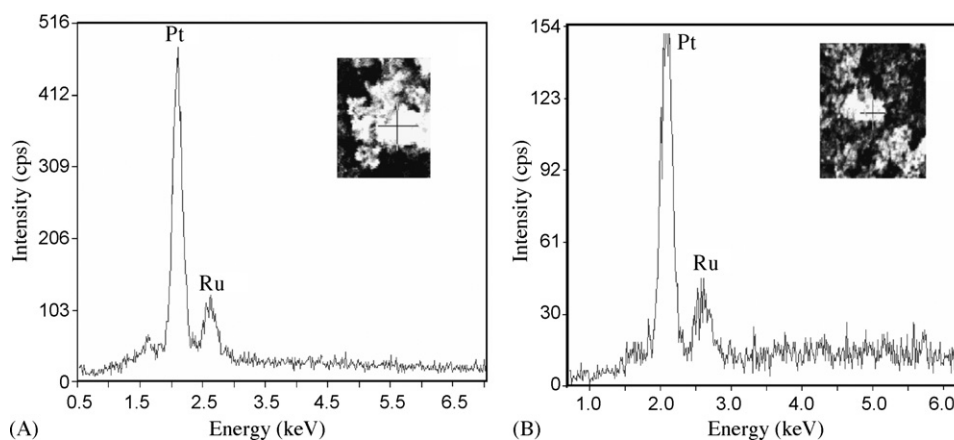


Fig. 3. EDAX patterns of Pt–Ru/C catalysts prepared from the acidic (A) and the alkaline (B) $\text{Pt}(\text{NH}_3)_2(\text{NO}_2)_2$ as precursors.

The average particle size d may be estimated from Pt (2 2 0) FWHM according to Debye–Scherrer formula [15]. The average particle sizes of Pt–Ru/C catalysts prepared from the acidic and the alkaline $\text{Pt}(\text{NH}_3)_2(\text{NO}_2)_2$ solutions are 3.7 and 5.8 nm, respectively.

Chemical compositions of the Pt–Ru/C catalysts were determined by EDAX analysis. Fig. 3 shows EDAX patterns of Pt–Ru/C catalysts prepared from the acidic (A) and the alkaline (B) $\text{Pt}(\text{NH}_3)_2(\text{NO}_2)_2$ solutions as precursors. Typical values of the composition analysis of them are shown in Table 1.

The EDAX analysis showed that the determined composition of Pt–Ru/C catalyst from the acidic $\text{Pt}(\text{NH}_3)_2(\text{NO}_2)_2$ solution as precursor was quite similar to the theoretical one of 1:1. The Pt and Ru composition ratio of Pt–Ru/C catalyst from the alkaline one is 6:4. It shows that the degree of alloying of catalyst from the acidic $\text{Pt}(\text{NH}_3)_2(\text{NO}_2)_2$ is higher than that of catalyst from the latter material.

3.2. Effect of precursors on dispersion of the catalysts

Fig. 4 shows the TEM micrographs of the Pt–Ru/C catalysts prepared from the acidic (A) and the alkaline (B)

$\text{Pt}(\text{NH}_3)_2(\text{NO}_2)_2$ solutions as Pt precursors. The dark black portions are Pt–Ru grains, and the grey portions are carbon black grains. It can be seen that the dispersion of the catalyst from the acidic $\text{Pt}(\text{NH}_3)_2(\text{NO}_2)_2$ as precursor is homogeneous. Its particle size is relatively small. The dispersion of the catalyst from the alkaline one as Pt precursor is inhomogeneous with a certain extent of agglomeration. The particle size of the catalyst is relatively big.

The values of Pt–Ru metal particle mean diameter are the number averaged diameters of the Pt–Ru particles in samples, which can be computed from TEM measurements of individual particle diameters, d_i , using the following equation [16]:

$$\bar{d}_n = \frac{\sum_{i=1}^n d_i}{n} \quad (1)$$

where \bar{d}_n is the number averaged diameter of Pt–Ru particles in nm. The mean particle sizes of Pt–Ru/C catalysts prepared from the acidic and the alkaline $\text{Pt}(\text{NH}_3)_2(\text{NO}_2)_2$ solutions are 3.6 and 6.0 nm, respectively. It is consistent with the particle sizes calculated from XRD patterns.

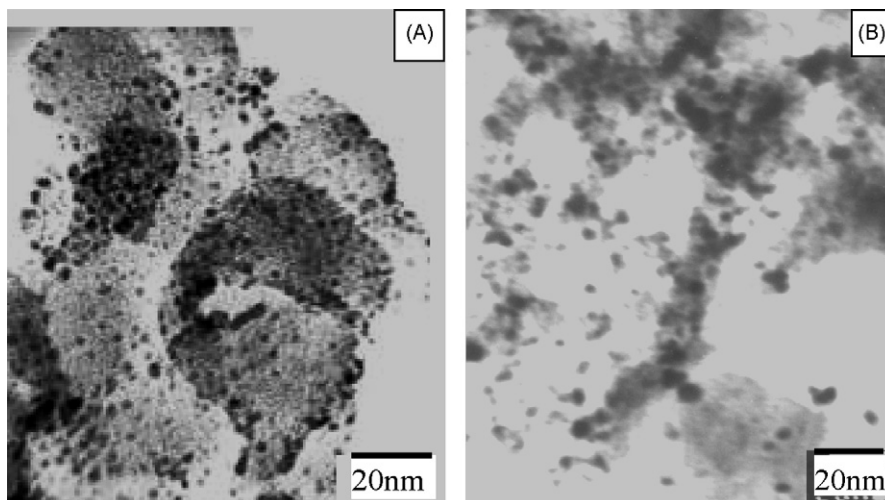


Fig. 4. TEM micrographs of Pt–Ru/C catalysts prepared from the acidic (A) and the alkaline (B) $\text{Pt}(\text{NH}_3)_2(\text{NO}_2)_2$ as precursors.

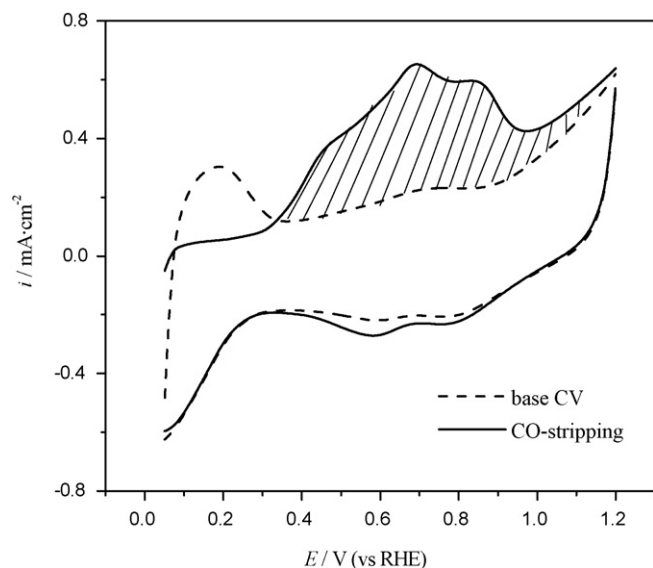


Fig. 5. CV curves for CO electrooxidation on the Pt–Ru/C catalysts prepared from the acidic $\text{Pt}(\text{NH}_3)_2(\text{NO}_2)_2$ as precursors in an Ar-saturated solution of $0.5 \text{ mol L}^{-1} \text{ H}_2\text{SO}_4$ at 25°C . Scan rate: 0.02 V s^{-1} .

3.3. Effect of precursors on specific area of the catalysts

The surface area (denoted as S_{XRD}) of the catalyst can be evaluated from the X-ray diffraction peaks using the following equations [17,18]:

$$S = \frac{6000}{\rho_{\text{Pt-Ru}} d} \quad (2)$$

$$\rho_{\text{Pt-Ru}} = X_{\text{Pt}} \rho_{\text{Pt}} + X_{\text{Ru}} \rho_{\text{Ru}} \quad (3)$$

where d is the average particle size (nm), $\rho_{\text{Pt-Ru}}$ the density of Pt–Ru alloy, ρ_{Pt} the density of Pt metal (21.4 g cm^{-3}), ρ_{Ru} the density of Ru metal (12.3 g cm^{-3}), and X_{Pt} and X_{Ru} are the weight percent of Pt and Ru, respectively, in the catalysts.

The electrochemically active surface areas (denoted as S_{EAS}) of the Pt–Ru/C catalysts are calculated by using Eq. (4) [19,20] and the cyclic voltammograms (CV) of CO adsorption and oxidation (area with oblique lines in Fig. 5). The results are shown in Table 2:

$$S_{\text{EAS}} = \frac{Q_{\text{CO}}}{G_{\text{Pt-Ru}} \times 420 (\mu\text{C/cm}^2)} \quad (4)$$

where Q_{CO} is the charge quantity for CO desorption electrooxidation in microcoulomb (μC), $G_{\text{Pt-Ru}}$ represents the Pt–Ru metal loading (μg) in the electrode, and $420 (\mu\text{C cm}^{-2})$ is the charge required to oxidize a monolayer of CO on Pt–Ru/C catalyst.

Table 2
Specific surface areas of the Pt–Ru/C catalysts prepared from the acidic and the alkaline $\text{Pt}(\text{NH}_3)_2(\text{NO}_2)_2$ as precursors

Precursors	Acidic $\text{Pt}(\text{NH}_3)_2(\text{NO}_2)_2$	Alkaline $\text{Pt}(\text{NH}_3)_2(\text{NO}_2)_2$
$S_{\text{XRD}} (\text{m}^2 \text{ g}^{-1})$	90.09	57.5
$S_{\text{EAS}} (\text{m}^2 \text{ g}^{-1})$	88.53	50.8

It can be seen from Table 2 that the S_{XRD} and the S_{EAS} of Pt–Ru/C catalyst from the same $\text{Pt}(\text{NH}_3)_2(\text{NO}_2)_2$ solution are almost the same. However, the S_{XRD} and the S_{EAS} of Pt–Ru/C catalyst from the alkaline Pt precursor are much smaller than that of from the acidic $\text{Pt}(\text{NH}_3)_2(\text{NO}_2)_2$ solution.

3.4. Effect of precursors on performance of the catalysts

Fig. 6 shows the cyclic voltammograms for the Pt–Ru/C catalysts prepared from different Pt precursors in a solution of $0.5 \text{ mol L}^{-1} \text{ CH}_3\text{OH}$ and $0.5 \text{ mol L}^{-1} \text{ H}_2\text{SO}_4$.

It can be seen from Fig. 6 that the onset potential of a current rise for methanol electrooxidation for the Pt–Ru/C catalyst prepared from the acidic $\text{Pt}(\text{NH}_3)_2(\text{NO}_2)_2$ solution corresponds to that for the catalyst obtained from the alkaline one, *i.e.* about 0.55 V . The potential for methanol electrooxidation, at which the peak current occurs, is 0.88 V (versus RHE), and the peak current density is 11.5 mA cm^{-2} during positive potential scanning on the Pt–Ru/C catalyst from the acidic $\text{Pt}(\text{NH}_3)_2(\text{NO}_2)_2$ solution as shown by curve A. The peak potential and the peak current density on the Pt–Ru/C catalyst are about 0.70 V (versus RHE) and 7.8 mA cm^{-2} , respectively, during its reverse scanning. The peak potential for methanol electrooxidation and the peak current density on the Pt–Ru/C catalyst from the alkaline one are about 0.89 V (versus RHE) and 6.1 mA cm^{-2} , respectively, during positive potential scanning as shown by curve B. The peak potential and the peak current density on the Pt–Ru/C catalyst are about 0.74 V (versus RHE) and 5.2 mA cm^{-2} , respectively, during its reverse scanning. The peak potential on the Pt–Ru/C catalyst from the acidic $\text{Pt}(\text{NH}_3)_2(\text{NO}_2)_2$ during potential scanning is 10 mV lower than that on the catalyst from the alkaline one. But the peak current density for the Pt–Ru/C catalyst from the acidic $\text{Pt}(\text{NH}_3)_2(\text{NO}_2)_2$ is 5.4 mA cm^{-2} higher than that for the catalyst from the alkaline one. So, the performance of Pt–Ru/C catalyst from the acidic $\text{Pt}(\text{NH}_3)_2(\text{NO}_2)_2$ solution for

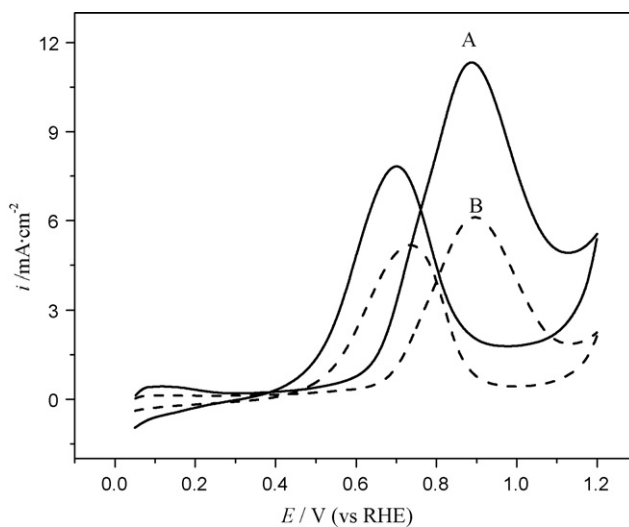


Fig. 6. Cyclic voltammograms of methanol electrooxidation in a solution of $0.5 \text{ mol L}^{-1} \text{ CH}_3\text{OH}$ and $0.5 \text{ mol L}^{-1} \text{ H}_2\text{SO}_4$ at 25°C on the Pt–Ru/C catalysts prepared from the acidic (A) and the alkaline (B) $\text{Pt}(\text{NH}_3)_2(\text{NO}_2)_2$ as precursors. Scan rate: 20 mV s^{-1} .

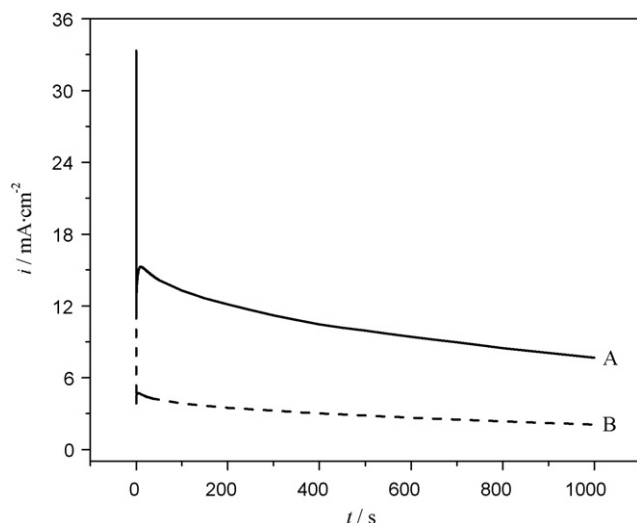


Fig. 7. Chronoamperometric curves of methanol electrooxidation in a solution of $0.5 \text{ mol L}^{-1} \text{ CH}_3\text{OH}$ and $0.5 \text{ mol L}^{-1} \text{ H}_2\text{SO}_4$ at 25°C on the Pt–Ru/C catalysts prepared from the acidic (A) and the alkaline (B) $\text{Pt}(\text{NH}_3)_2(\text{NO}_2)_2$ as precursors. Potential jumps from 0.1 to 0.8 V.

methanol electrooxidation is much better than that for the catalyst from the latter material.

The activities for methanol electrooxidation measured as steady-state current densities at constant potential were used to compare the performance of our electrocatalysts prepared from different precursors. Fig. 7 shows the current densities measured at a constant potential jumping from 0.1 to 0.8 V in an Ar-saturated solution of $0.5 \text{ mol L}^{-1} \text{ CH}_3\text{OH}$ and $0.5 \text{ mol L}^{-1} \text{ H}_2\text{SO}_4$ at 25°C . The initial high current densities correspond mainly to double-layer charging. The currents decay with time in the parabolic style and reach an apparent steady state within 500 s. It can be seen that the current of methanol electrooxidation for the Pt–Ru/C catalyst prepared from the acidic $\text{Pt}(\text{NH}_3)_2(\text{NO}_2)_2$ solution is the higher one at the same potentials, *i.e.* its catalytic activity and the stability of the catalyst prepared from it for methanol electrooxidation is better. The current on the catalyst prepared from the alkaline $\text{Pt}(\text{NH}_3)_2(\text{NO}_2)_2$ is relatively small, *i.e.* its performance is the lower one. The results are similar to those of cyclic voltammetry measurement.

The $\text{Pt}(\text{NH}_3)_2(\text{NO}_2)_2$ compounds may have two configurations: one is *cis*-structure [21], difficult to dissolve in water, easy to dissolve in ammonium hydroxide and form the colorless alkaline solution with the pH value of about 11.6. The other is yellow crystalline powder, easy to dissolve in water and form the yellow acidic solution with the pH value of about 1.5. The pH value of the acidic Ru compound solution used is about 2.3. The pH value of the mixture ink of the acidic platinum, ruthenium compounds precursors, and carbon is about 1.8. However, the pH value of the alkaline one, the acidic Ru solution, and carbon mixture ink is about 7.5. An acidic and alkaline neutralization reaction can occur which destroys the environments that they dissolved, respectively, when the alkaline $\text{Pt}(\text{NH}_3)_2(\text{NO}_2)_2$ and the acidic Ru solution are added to the carbon ink during catalyst preparation. The solubility of $\text{Pt}(\text{NH}_3)_2(\text{NO}_2)_2$ compound decreases

and its crystal is evolved. The precipitation of $\text{Ru}(\text{OH})_3$ is formed from Ru compound. The amount of $[\text{Pt}(\text{NH}_3)_2]^{4+}$ and Ru^{3+} ions adsorbed in carbon surface decreases, and the $\text{Pt}(\text{NH}_3)_2(\text{NO}_2)_2$ crystal evolves and $\text{Ru}(\text{OH})_3$ precipitation exists independently in solid powder which consists of the Pt, Ru compounds and carbon. So, the chemical composition of Pt and Ru in the Pt–Ru/C catalyst is deflected from the theoretical value of 1:1. The electrocatalytic activity of the Pt–Ru/C catalyst for methanol electrooxidation decreases. The environments of strong acidity (the pH value of 1.8), which they dissolved, respectively, can be kept when the acidic $\text{Pt}(\text{NH}_3)_2(\text{NO}_2)_2$ solution and the acidic Ru solution are added to the carbon ink. The $[\text{Pt}(\text{NH}_3)_2]^{4+}$ and Ru^{3+} ions can be evenly adsorbed in carbon support. So, the particle size of the Pt–Ru/C catalyst prepared from the acidic $\text{Pt}(\text{NH}_3)_2(\text{NO}_2)_2$ solution is relatively small, and its distribution is homogeneous in carbon. Its chemical composition is quite similar to the theoretical one of 1:1. Its performance is higher than that from the alkaline $\text{Pt}(\text{NH}_3)_2(\text{NO}_2)_2$ as Pt precursor. So, it needs to be taken into account matching of precursors used before the alloy catalysts are prepared.

4. Conclusions

Electrocatalytic activity of the Pt–Ru/C catalyst which was formed by thermal reduction with the acidic and the alkaline $\text{Pt}(\text{NH}_3)_2(\text{NO}_2)_2$ solutions, respectively, and the same acidic Ru compound as precursors, was investigated with respect to the electrooxidation of methanol in H_2SO_4 solution. The experimental data reported in this paper indicate that the performance of the Pt–Ru/C catalyst prepared from the acidic $\text{Pt}(\text{NH}_3)_2(\text{NO}_2)_2$ solution as the Pt precursor for methanol electrooxidation is better than that of the catalyst from the alkaline solution due to the acidic environment of the precursor ink with the acidic $\text{Pt}(\text{NH}_3)_2(\text{NO}_2)_2$ and the acidic Ru compound as precursors, and the forming of a homogeneous dispersion of Pt–Ru metal particles with relatively small sizes on the carbon support.

References

- [1] J.-H. Choi, K.-W. Park, I.-S. Park, W.-H. Nam, Y.-E. Sung, *Electrochim. Acta* 50 (2004) 787.
- [2] Z.B. Wang, G.P. Yin, P.F. Shi, *Carbon* 44 (2006) 133.
- [3] T. Yamaguchi, H. Kuroki, F. Miyata, *Electrochem. Commun.* 7 (2005) 730.
- [4] F.J. Rodriguez-Nieto, T.Y. Morante-Catacora, C.R. Cabrera, *J. Electroanal. Chem.* 571 (2004) 26.
- [5] J.S. Guo, G.Q. Sun, Q. Wang, G.X. Wang, Z.H. Zhou, S.H. Tang, L.H. Jiang, B. Zhou, Q. Xin, *Carbon* 44 (2006) 152.
- [6] Y.M. Liang, H.M. Zhang, B.L. Yi, Z.H. Zhang, Z.C. Tan, *Carbon* 43 (2005) 3144.
- [7] M.-K. Min, J. Cho, K. Cho, H. Kim, *Electrochim. Acta* 45 (2000) 4211.
- [8] K. Lasch, L. Jorissen, J. Garcke, *J. Power Sources* 84 (1999) 225.
- [9] X. Zhang, K.-Y. Chan, *Chem. Mater.* 15 (2003) 451.
- [10] Z.B. Wang, G.P. Yin, P.S. Shi, *Battery Bimonthly* 35 (2005) 70.
- [11] B. Bachiller-Baeza, A. Guerrero-Ruiz, I. Rodriguez-Ramos, *Appl. Catal. A: Gen.* 192 (2000) 289.
- [12] M. Watanabe, M. Uchida, S. Motoo, *J. Electroanal. Chem.* 229 (1987) 395.
- [13] Z.B. Wang, G.P. Yin, P.F. Shi, *Acta Phys.-Chim. Sin.* 21 (2005) 1156.

- [14] T.J. Schmidt, H.A. Gasteiger, G.D. Stab, P.M. Urban, D.M. Kolb, R.J. Behm, J. Electrochem. Soc. 145 (1998) 2354.
- [15] L. Giorgi, A. Pozio, C. Bracchini, R. Giorgi, S. Turtu, J. Appl. Electrochem. 31 (2001) 325.
- [16] P.J. Ferreira, G.J. Ia, O.Y. Shao-Horn, D. Morgan, R. Makharia, S. Kocha, H.A. Gasteiger, J. Electrochem. Soc. 152 (2005) A2256.
- [17] Z.B. Wang, G.P. Yin, P.F. Shi, J. Electrochem. Soc. 152 (2005) A2406.
- [18] C.Z. He, H.R. Kunz, J.M. Fenton, J. Electrochem. Soc. 144 (1997) 970.
- [19] A. Pozio, M.D. Francesco, A. Cemmi, F. Cardellini, L. Giorgi, J. Power Sources 105 (2002) 13.
- [20] Z.B. Wang, G.P. Yin, P.F. Shi, Y.C. Sun, Electrochem. Solid-State Lett. 9 (2006) A13.
- [21] C.R.K. Rao, D.C. Trivedi, Coord. Chem. Rev. 249 (2005) 613.